American Mineralogist, Volume 80, pages 982–997, 1995

Phlogopite stability in the silica-saturated portion of the system $KAlO_2$-MgO-SiO_2-H_2O: New data and a reappraisal of phase relations to 1.5 GPa

JOHN D. CLEMENS
School of Geological Sciences, Kingston University, Penrhyn Road, Kingston-upon-Thames, Surrey KT1 2EE, U.K.

ABSTRACT

Phlogopite-quartz stability in the system $KAlO_2$-MgO-SiO_2-H_2O represents a simple model for the stability of biotite in many common, crustal rock types during granulite-facies metamorphism and in the crystallization of intermediate to felsic magmas. Despite many previous experimental and theoretical topological studies, disagreement remains on the stoichiometries and P-T locations of many of the six equilibria emanating from the invariant point at which phlogopite, β-quartz, high sanidine, orthoenstatite, aqueous fluid, and hydrous alumino-silicate melt coexist. In their experimental and modeling study, Vielzeuf and Clemens (1992) resolved most of the disagreement among data sets for the fluid-absent melting reaction Phl + Qtz = En + Sa + M (Fl). The five remaining equilibria form the main subject of this paper:

$$\text{Phl} + 3\text{Qtz} = 3\text{En} + \text{Sa} + \text{H}_2\text{O} \quad \text{(M)}$$
$$\text{Phl} + \text{Qtz} + \text{Sa} + \text{Fl} = \text{M} \quad \text{(En)}$$
$$\text{En} + \text{Qtz} + \text{Sa} + \text{Fl} = \text{M} \quad \text{(Phl)}$$
$$\text{Phl} + \text{Qtz} + \text{Fl} = \text{En} + \text{M} \quad \text{(Sa)}$$
$$\text{En} + \text{Sa} + \text{Fl} = \text{Phl} + \text{M} \quad \text{(Qtz).}$$

Previous data on the equilibria are reevaluated, and I present further experimental constraints showing that the data sets are mostly reconcilable and that some seeming contradictions result from misinterpretations of the experimental products in relation to the compositions of the starting materials. I present the most accurate possible depiction of the P-T topological relations, given our current knowledge of the system.

The very tight experimental constraints on the locus of reaction (M) make it possible to refine the value for the free energy of formation of Al-Si–disordered phlogopite, reducing the uncertainty on the calorimetrically determined value (Clemens et al., 1987) by 46%. The new value for ΔG_f^0 Phl is -5838.16 ± 3.37 kJ/mol.

Contrary to the conclusions of some previous studies, reactions (Sa) and (En) are nowhere near coincident. The (Sa) reaction exhibits graceful slope changes that vary in sympathy with those for (Fl). The ultimate controls on this are probably subtle variations, with pressure, of the partial molar volume and entropy of H_2O in the hydrous alumino-silicate melt.

Reaction (Qtz) probably has a slightly negative (almost flat) dP/dT slope, with melt on the high-T side, which seems more logical than previous depictions of the reaction with a positive slope and melt on the low-T side.

Melt MgO contents are always very low. Thus, although reactions (En) and (Phl) lie at lower T than Sa + Qtz + Fl = M, the amount of solidus depression due to the presence of MgO is very small.

If (Fl) is taken as a model for fluid-absent biotite breakdown in quartzofeldspathic rocks and metagraywackes at granulite grade, its constant positive or infinite dP/dT slope would allow adiabatic ascent of the melt to very high crustal levels. This agrees with the inferred origin of many granitoids and silicic volcanic complexes. On the other hand, many migmatites have formed through fluid-saturated partial melting reactions in the amphibolite-facies middle crust. If this occurred by reactions similar to (Sa), the negative dP/dT slopes of such equilibria would seem to prohibit magma ascent. However, if the natural reactions

0003–004X/94/0910–0982$02.00

exhibit slope changes similar to that of (Sa), it may be possible for some H_2O-saturated melts formed by biotite breakdown to ascend significant distances without crossing their solidi.

Finally, experimental and thermodynamic constraints suggest that the anthophyllite dehydration reaction (Ant = 7En + Qtz + H_2O) intersects reaction (Sa) at between 600 and 700 MPa. This would render (Sa) metastable and introduce new equilibria. The talc dehydration reaction (7Tc = 3Ant + 4Qtz + $4H_2O$) also appears likely to intersect one of these, at some pressure above 800 MPa, introducing further complications. Though they are likely to be stable, none of these new talc and anthophyllite melting equilibria have been encountered experimentally. This is almost certainly a consequence of the huge kinetic barrier to the crystallization of anthophyllite and may mean that it is impossible to determine experimentally the complete stable phase diagram. However, this is a problem peculiar to experimental studies in $KAlO_2$-MgO-SiO_2-H_2O and does not detract from the usefulness of the metastable equilibria for modeling petrogenetic processes because the talc and anthophyllite equilibria are unlikely to interfere in natural Fe-bearing systems.

Introduction

Despite numerous experimental and theoretical topological studies (e.g., Luth, 1967; Wood, 1976; Wones and Dodge, 1977; Bohlen et al., 1983; Grant, 1986; Ostapenko et al., 1987; Peterson and Newton, 1989; Montana and Brearley, 1989), disagreement remains on the stoichiometries and *P-T* locations of many equilibria involving phlogopite breakdown in the silica-saturated portion of the system $KAlO_2$-MgO-SiO_2-H_2O. The following six equilibria all emanate from an invariant point (I_1 in Fig. 1) that involves phlogopite (Phl), quartz (Qtz), sanidine (Sa), enstatite (En), aqueous fluid (Fl), and silicate melt (M): the subsolidus reaction Phl + 3Qtz = 3En + Sa + H_2O (M); the fluid-present, incongruent melting reaction Phl + Qtz + Fl = En + M (Sa); the congruent melting reactions Phl + Qtz + Sa + Fl = M (En) and En + Qtz + Sa + Fl = M (Phl); the fluid-absent melting reaction Phl + Qtz = En + Sa + M (Fl); and the quartz-absent reaction En + Sa + Fl = Phl + M (Qtz).

Vielzeuf and Clemens (1992) resolved most of the disagreement among data sets for the fluid-absent melting reaction, offering explanations for the apparently contradictory results in previous investigations. They showed that sanidine is a product (and not a reactant) in (Fl), over a wide range of pressure. They also concluded that, at pressures very near the invariant point (I_1), there may exist several other minor equilibria generated by the occurrence of phase colinearities. These complications appear to be geologically irrelevant. The five remaining equilibria are the main subject of this paper, though I report the result of one additional fluid-absent experiment at 500 MPa and no new constraints on the phlogopite-absent reaction (Phl), which occurs at very low pressures. For some background to the controversies associated with these equilibria see Helgeson et al. (1978), Bohlen et al. (1983), Montana and Brearley (1989), Vielzeuf and Clemens (1992), and Grant (1986).

Interest in this system stems from the fact that it represents a simple model for the stability and behavior of biotite in some common, crustal rock types under conditions appropriate to granulite-facies metamorphism or crystallization of intermediate to felsic magmas. If the relevant phase relations were accurately known, then phlogopite stability in this system could ultimately provide the basis for rigorous calculation of f_{H_2O} and modeling of subsolidus and melting equilibria in high-grade metamorphism, anatexis, and magma crystallization. The other barrier to achieving this goal is the fact that mixing properties for the end-members in complex mica solid solutions remain essentially unknown.

Recent calorimetric investigations (Robie and Hem-

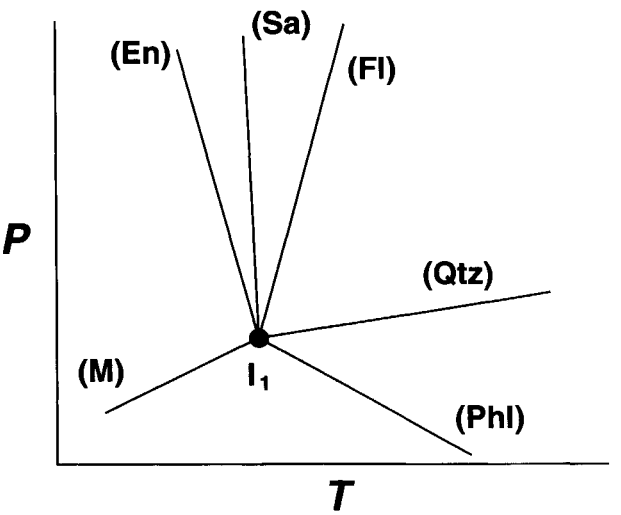

Fig. 1. Pressure-temperature phase diagram showing a theoretical distribution of univariant equilibria around the invariant point (I_1) at which phlogopite, quartz, enstatite, sanidine, melt, and aqueous fluid coexist in the system $KAlO_2$-MgO-SiO_2-H_2O. Equilibria are labeled according to the phase that does not participate. The positions and relative slopes of the reactions are approximately consistent with previous experimental work and theoretical treatments. Note that, in the immediate neighborhood of I_1, Vielzeuf and Clemens (1992) suggested that there exist two singular points and the additional equilibria Phl + Qtz = En + M + Fl, Phl + Qtz + Sa = En + M, and Phl + Qtz = En + M, all at a pressure of <100 MPa. This minor complication arises because reaction (M) intersects the wet solidus at a pressure so low that the melt formed in reaction (Sa) is initially unable to dissolve all the H_2O contained (as OH^-) in the phlogopite.

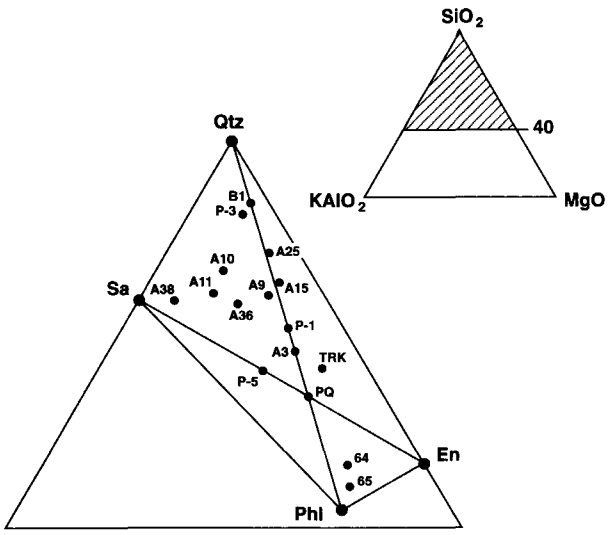

Fig. 2. The upper portion of the triangular diagram SiO_2-$KAlO_2$-MgO (shaded area in inset) with the positions of Qtz, Phl, Sa, and En plotted and showing the compositions of some of the starting materials used in this and previous experimental studies, as referred to in the text. Compositions P-1, P-3, and P-5: present work; 64 and 65: Luth (1967); PQ, TRK, A3, A9, A10, A11, A15, A25, A36, and A38: Wones and Dodge (1977).

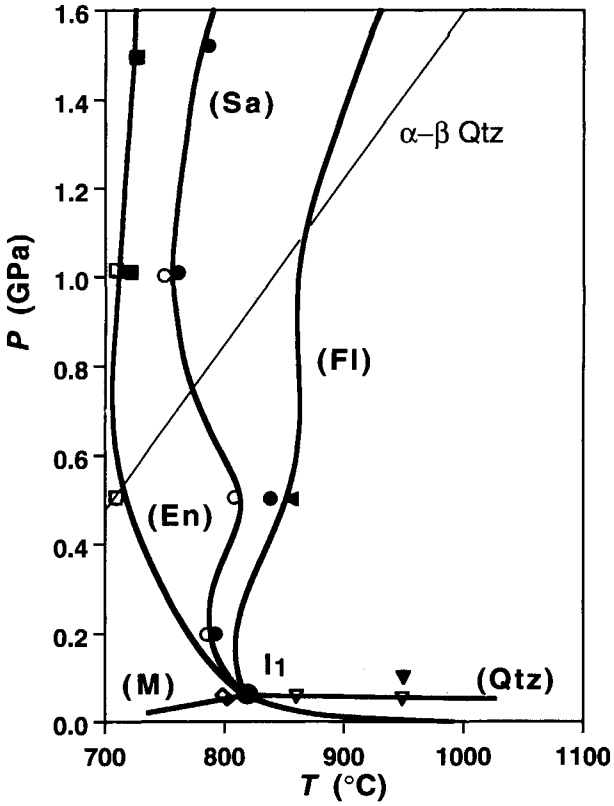

Fig. 3. *P-T* phase diagram showing the actual positions and shapes of the six major equilibrium boundaries under discussion. Equilibria are labeled according to the absent phase; I_1 is the invariant point. Data come from the present work and include the consistent data of all previous studies (see text and Tables 1 and 2). Constraints from the present work are indicated with open symbols for the low-*T* side and solid symbols for the high-*T* side. Symbols are: (M) = diamonds, (En) = squares, (Sa) = circles, (Fl) = left-pointing triangle, and (Qtz) = downward-pointing triangle.

ingway, 1984; Clemens et al., 1987; Circone and Navrotsky, 1992) have yielded thermodynamic data for phlogopite that are consistent with the best published experimental results on the subsolidus equilibrium (M) (Wood, 1976; Bohlen et al., 1983). The purpose of the present work is to evaluate critically previous data on phlogopite stability and to present further experimental constraints. In so doing, I will show that the several sets of data are, for the most part, reconcilable, and that some apparent contradictions result from misinterpretations of the experimental products in relation to the compositions of the starting materials. I will present what I believe to be the currently most accurate possible depiction of the *P-T* topological relations among the six equilibria. I will then discuss some of the implications for granulites, migmatites, melt mobility, and biotite stability in granitoid magmas. The final section deals with the probability that (Sa) becomes metastable with respect to anthophyllite and talc equilibria above about 600 MPa.

Previous H_2O-saturated experiments

There have been several previous experimental investigations of the equilibria surrounding invariant point I_1 in Figure 1. Data presented below indicate that these reactions are probably truly univariant in character. I have critically examined the published data to determine what constraints can be placed on the locations of these equilibria in *P-T* space. This section reviews the results of various studies, in chronological order, paying particular attention to the compositions of starting materials (Fig. 2) and how these affect interpretation of the experimental results. Table 1 lists the constraints used in construction of the final phase diagram of Figure 3. Note that quoted temperature uncertainties are generally due to observed variations over the course of an experiment. Absolute uncertainty (because of thermocouple calibration) may be highly variable and is not always known. Thus, I have judged experiment consistency purely on the basis of the published variability in measured experimental *T*. The reader should bear in mind that a further, absolute uncertainty of no more than 10 °C may apply to all quoted temperatures, including those for the present work.

Luth (1967)

Luth tabulates the results of 462 H_2O-saturated experiments on 37 different compositions in the system. Experiments were performed in cold-seal and internally heated vessels with Ar pressure media. Temperatures were read with type-S (Pt-PtRh10%) thermocouples and are

TABLE 1. Constraints from previous studies

Reaction	P (MPa)	T (°C)	Reference	Comments
(M)	25 ± 0.7	<755	1	
	37 ± 0.7	<795	1	
*	39.3–47.7	790 ± 5	1	
*	29.3–35.7	750 ± 5	1	
	20 ± 0.1	<724	2	
	40 ± 0.2	<775	2	
	30	<750	3	
	32	<773	3	
	34	>710	3	
	36	>761	3	
	40	<785	3	
	44.5	<795	3	
	49	>790	3	
(Phl)	40	>815	2	PQ produced En + Sa, no melt
	50	<833	2	A36 produced melt
(En)	50	<790	3	inconsistent, below solidus
	100	795–803	2	
	200 ± 1	757–775	2	
	200	740–760	3	
	500	<723	3	
	700	<708	3	
*	1000	700–720	3	
*	1500	719–730	3	reversal 709–739 °C
(Sa)	160	<813	3	
	193 ± 7.5	<810	4	
	200 ± 1	<781	2	inconsistent
	230	<800	3	
	320	<795	3	
	500	730–740	5	inconsistent
*	500	785–810	3	consistent if T error = 5 °C
	750	710–720	5	inconsistent
	1000	700–720	5	inconsistent
	1000	780–790	3	inconsistent
*	1000	780–810	3	inconsistent
	1000	720–730	6	inconsistent
	1350	<805	3	
	1450	<795	3	
	1500	750–760	5	inconsistent
*?	1500	770–800	3	inferred from 1550 MPa expt.
(Qtz)	33.9–76.4	900 ± 10	4	
	>49.7	839 ± 2	2	
	<50.3	840 ± 2	2	

Note: Reference 1 = Wood (1976), 2 = Wones and Dodge (1977), 3 = Peterson and Newton (1989), 4 = Luth (1967), 5 = Bohlen et al. (1983), and 6 = Montana and Brearley (1989).
* Reversal experiment.

quoted as accurate to ±10 °C. Pressures are given to ±7.5 MPa. Starting materials were synthesized from gels. Most of the studied compositions are silica-undersaturated, but 64 and 65 fall in the sanidine + phlogopite + enstatite field in Figure 2 and can be used to constrain the quartz-absent reaction (Qtz). Because the compositions are also in the quartz + phlogopite + enstatite field, they can be used to constrain reaction (Sa) by the appearance or non-appearance of melt at pressures above the invariant point I_1. Table 1 shows the results.

Wood (1976)

Wood used stoichiometric mixtures of synthetic phlogopite, quartz, enstatite, and sanidine (1:3:3:1 molar ratio) to locate the subsolidus dehydration reaction (M) at very low pressures. X-ray diffraction techniques were used to identify changes in mineral proportions between starting materials and experimental products. Cold-seal vessels were used, with H_2O pressure media, and all charges contained excess H_2O. Pressures are quoted to ±0.7 MPa and temperatures to ±5 °C. Wood notes that, at T > 800–810 °C, melting occurred at both 50 and 100 MPa. This agrees with Wones and Dodge's (1977) constraints on solidus reactions (Phl) and (En) (see below).

For reaction (M), Wood obtained constraints (at 25 and 37 MPa) and reversals at 750 and 790 °C. Within experimental errors, these are consistent with other data, including the calorimetric value of ΔG_f°Phl (Clemens et al., 1987). Note that these last authors erroneously stated the contrary.

Wones and Dodge (1977)

The experiments of Wones and Dodge were performed on nine compositions, all within the sanidine + enstatite + quartz field in Figure 2. Starting materials were synthesized from glasses and gels. Phlogopite was crystallized hydrothermally and mixed with gem-quality Brazilian quartz to form starting material PQ. Composition

TRK was a mixture of synthetic, crystalline tremolite, sanidine, diopside, phlogopite, and quartz. This composition (TRK) is also plotted on Figure 2, projected from CaO. All starting compositions were hydrothermally precrystallized, but some of these final starting materials contained glass or unreacted gel.

For the experiments, starting mixes were loaded into Au capsules and sealed with excess H_2O. Temperatures were measured with internal, type-K (chromel-alumel) thermocouples calibrated against the 1 atm melting point of NaCl (801 °C). Pressure was monitored with Bourdon tube gauges and is quoted to ±0.5% (relative). Experimental products were identified with optical and X-ray diffraction methods.

Compositions A9, A10, A11, A36, and A38 fall in the sanidine + phlogopite + quartz field and are thus suitable for determining the position of the solidus reaction [(Phl) or (En)]. At pressures lower than invariant point I_1 in Figure 1, mixtures of phlogopite + quartz with molar ratios of phlogopite to quartz < 1:3 decompose to mixtures of sanidine, enstatite, and quartz prior to any melting. Thus, Wones and Dodge's compositions A3, A15, and A25 can also be used to constrain the solidus reaction (Phl). Wones and Dodge incorrectly interpreted the results of experiments on compositions A9, A36, and A38 as providing constraints on reaction (Sa). Because these compositions plot on the sanidine side of the quartz-phlogopite join in Figure 2, they cannot be used to delineate reaction (Sa); the first melt is always produced at the solidus reaction [(Phl) or (En)]. The occurrences of En in the products of experiments on A36 and A38, as well as other compositions, are all consistent with (Sa) being at slightly higher T than (En) at these low pressures. This is consistent with the present and other recent results (see below). The critical experiment involved composition A15, at 200 MPa and 780 ± 1 °C, which contained En in its products. This implied that (Sa) remains close to (En) at higher P also. However, composition A15 plots on the En side of the quartz-phlogopite join in Figure 2, containing a small amount of excess enstatite. Therefore, appearance of this phase in the experimental product does not indicate that reaction (Sa) has occurred. Erroneous attribution of these data resulted in the long-standing misconception that reactions (En) and (Sa) are nearly coincident over a large P range (see Bohlen et al., 1983; Grant, 1986).

Compositions PQ, A3, A15, and A25 can be used to constrain the fluid-present melting reaction (Sa) by noting the first appearance of glass as an experimental product (or glass and enstatite for PQ and A3). Note that results on composition TRK cannot be used because of the occurrence of the competing reaction Phl + Di + Qtz = Tr + M at lower T than reaction (Sa) (Wones and Dodge, 1977).

The quartz-absent melting reaction (Qtz) can be located using the results on composition PQ if the starting material contained no phlogopite (only sanidine and enstatite). Two such experiments were conducted by Wones and Dodge.

Lastly, the results place limits on the location of subsolidus reaction (M). Compositions PQ, A3, A15, and A25 are suitable. One experiment provides an upper temperature limit on (M) because sanidine and enstatite grew at the expense of phlogopite + quartz in the absence of melt. Two other experiments provide an apparent bracket at 50 MPa. One additional experiment on composition TRK, gives an upper temperature limit. The products of this experiment contain sanidine, enstatite, and diopside grown from a starting mixture of tremolite, phlogopite, diopside, sanidine, and quartz. This means that the experiment was at a temperature higher than both reaction (M) and the reaction Phl + 2Di + 4Qtz = Tr + Sa (see Fig. 3 of Wones and Dodge, 1977). However, no reversals can be inferred, and one experiment is inconsistent with other data (see Table 1).

As a final note, one experiment, on composition PQ at 830 ± 3 °C and 50 MPa, is either inconsistent with the rest or used a capsule that leaked. The latter seems to be the most probable explanation because no reaction was observed, yet the experiment was clearly at supersolidus T and on the En side of reaction (M), according to the present results and the phase diagram of Wones and Dodge (1977, Fig. 2). This experiment was not used in construction of Figure 3, nor is it included in Table 1, because it appears to constrain none of the equilibria.

Bohlen, Boettcher, Wall, and Clemens (1983)

Bohlen et al. (1983) report experimental results on reactions (M), (Sa), and (Fl). For the starting materials, sanidine and enstatite were synthesized from gels, ground under acetone, and dried at 800 °C for 24 h. Brazilian quartz was finely ground, leached in HNO_3, and fired at 800 °C for 48 h. Phlogopite was prepared from K_2CO_3, MgO, Al_2O_3, and SiO_2, reacted hydrothermally. H_2O was boiled, doubly distilled, deionized water. The experimental apparatus is a 2.54 cm piston cylinder used with NaCl pressure cells and graphite tube furnaces. Calibration methods are detailed in Bohlen and Boettcher (1982), and I estimate P and T uncertainties to have been about ±20 MPa and ±3 °C.

Actual starting materials were mixtures of phlogopite and quartz (1:5 molar ratio) for melting experiments on reactions (Sa) and (Fl). This composition is plotted as B1 in Figure 2. Note that it lies on the phlogopite-quartz join (with neither excess sanidine nor excess enstatite). This means that solidus reaction (En) could not, therefore, have been located using these starting materials. The first melting, above invariant point I_1, would take place on either reaction (Sa) or (Fl), depending on the presence or absence of free H_2O in the charge.

Bohlen et al. state (p. 275) that their results for reaction (Sa) "join smoothly with the data of Wones and Dodge (1977)." As discussed above, Wones and Dodge (1977) obtained no brackets on reaction (Sa). Instead, they constrained reaction (En) because their critical starting materials were saturated in sanidine or enstatite. It could be argued that the phlogopite used by Bohlen et al. might

have had a minor sanidine impurity, unnoticed in X-ray examination, and that initial melting occurred at (En). However, this seems unlikely. At any given P, reaction (En) must lie at lower T than the solidus of the MgO-free analogue system (Sa + Qtz + Fl = M). Bohlen et al. give tight brackets for this reaction, and such an interpretation of their results would unequivocally place reaction (En) at higher T. Furthermore, Bohlen et al. note the appearance of enstatite in their experimental products. Enstatite would not have occurred if melting had been by the enstatite-absent reaction (En). These internal and external inconsistencies (see the discussion of data from Wones and Dodge, 1977, and Peterson and Newton, 1987) lead me to conclude that the Bohlen et al. results for reaction (Sa) are spurious.

Just as there are discrepancies between the results for (Sa) and other determinations, so there are major differences in the location of the fluid-absent melting reaction (Fl). The reasons for this have been discussed by Vielzeuf and Clemens (1992).

Ostapenko, Gorogotskaya, Timoshkova, and Yakovlev (1987)

The experiments of Ostapenko et al. (1987) dealt mostly with the analogue of subsolidus reaction (M) using complex, natural biotite and orthopyroxene starting compositions. However, some short (8 d) experiments were conducted with pure, synthetic phlogopite, enstatite, sanidine, and quartz. Experiments were performed in cold-seal vessels with f_{O_2} buffered by Ni + NiO + H_2O, and samples were encapsulated in Au or Pt. Actual results are not given, but Ostapenko et al. write that reaction (M) probably occurs at temperatures about 40 °C lower than shown in Figure 2 of Wones and Dodge (1977). This result agrees with the present assessment.

Peterson and Newton (1989)

More recent data on phlogopite + quartz reactions were obtained by Peterson and Newton (1989), including the tables lodged with the *Journal of Geology* Data Repository. These experiments used synthetic starting materials and were performed in internally heated vessels and a piston-cylinder apparatus with NaCl cells. Peterson and Newton used slightly nonstoichiometric, synthetic, 1 M phlogopite, synthetic high sanidine, and natural quartz. For investigation of reactions (M) and (Sa) they used phlogopite + quartz mixes (2:3 or 3:2 by weight) and for (En), phlogopite + quartz + sanidine mixes (2:3:2 by weight). Mixes were sealed in Au or Pt capsules with 20–50 wt% distilled water. They report half-brackets, brackets, and a reversal on solidus reaction (En) at pressures of 50, 200, 500, and 700 MPa, and 1 and 1.5 GPa. Reversal attempts were obtained in two-stage experiments. In the first stage, T was held for ~200 h at the point where melting was previously observed. In the second state, T was lowered and maintained for a further 200 h. These results are all consistent with the present work, except for their 50 MPa point [(En) at T < 790 °C)], which is discrepant with all other data. This experimental point lies about 25 °C below the solidus and disagrees with their own data for (M), located at >790 °C at MPa (see Table 1).

For the fluid-present reaction (Sa), they present half-brackets and reversals at several pressures between 160 MPa and 1.8 GPa. The present data (see below) essentially confirm the positions of these equilibria at pressures up to 320 MPa. Their 500 MPa bracket could be consistent if a small temperature measurement error (~5 °C) is accepted as possible. Their 1 GPa bracket places the reaction about 25 °C lower than in the present work. Finally, at 1.5 GPa their inferred reversal is consistent with the present work. The bracket quoted in the paper (Peterson and Newton, 1989) is inconsistent. However, the data in tables deposited with the *Journal of Geology* actually yield a broader bracket, consistent with the present results. In summary, the Peterson and Newton results for (Sa) are broadly consistent with the results obtained here.

Peterson and Newton reported experimental constraints on the fluid-absent reaction (Fl). Vielzeuf and Clemens (1992) discussed these results at length and produced what they believed to be the best possible resolution of the inconsistencies for the various sets of data on this reaction. The reader is referred to this work for further information.

The 1989 paper also contains data constraining the position of the subsolidus dehydration reaction (M). The results of the seven constraining experiments are consistent with all previous data (Wood, 1976; Wones and Dodge, 1977) and the present work (see below).

In addition, Peterson and Newton investigated the effects of removing H_2 from the system and isolating their samples from H_2 flux during experiments. This was done by placing H_2 getters, such as powdered hematite or borosilicate glass, around the capsules. They concluded that variations in f_{H_2}, at low levels, do not affect the positions of fluid-present reactions (En) and (Sa) but suggest that the temperature of the fluid-absent reaction (Fl) might be lowered by the presence of H_2. However, they present no experimental evidence bearing on this possibility.

Experimental details for the present study

The results of the present experiments are presented in Table 2. The sections below explain the methods used in the experiments and in the analysis and interpretation of results.

Apparatus

Experiments at $P \leq 200$ MPa. Most of the lower-pressure experiments were performed (at Department of Geology, University Blaise Pascal, Clermont-Ferrand) in cold-seal vessels with vertically mounted furnaces and used N_2 as the pressure medium. Temperatures were measured with external, type-S thermocouples and are believed accurate to ±2 °C. Thermal gradients were measured with an internal, type-K thermocouple at 1 atm and 800 °C. These amounted to <1 °C over 2 cm at the sam-

TABLE 2. Summary of experimental results from the present work

Expt.	P (MPa)	T (°C)	$X^{Fl}_{H_2O}$	t (h)	Starting material	Assemblage
			Reaction (M)			
K-22	51.0 ± 0.3	800 ± 2	1.00	383	P-5	En + Sa
K-23	51.0 ± 0.3	800 ± 2	1.00	383	P-1	Phl + Qtz + En + Sa
K-37	61.1 ± 0.6	800 ± 2	1.00	362	P-5	Phl(tr) + En + Sa
K-2	101 ± 1	769 ± 3	1.00	404	P-1	Phl + Qtz
			Reaction (En)			
K-114	506 ± 2	710 ± 1	1.00	163	P-3	Phl(m) + Qtz + Sa
K-79	1015 ± 14	710 ± 1	1.00	124	P-3	Phl(m) + Qtz + Sa
K-81	1011 ± 24	720 ± 1	1.00	97	P-3	Phl(m) + Qtz + Sa + Gl(m)
K-107	1499 ± 7	725 ± 1	1.00	122	P-3	Phl(m) + Qtz(tr) + Sa + Gl
			Reaction (Sa)			
K-8	200 ± 1	779 ± 1	1.00	287	P-1	Phl + Qtz
K-16	199 ± 1	786 ± 1	1.00	280	P-1	Phl + Qtz
K-9	200 ± 1	791 ± 1	1.00	287	P-1	Phl + Qtz + En(m) + Gl(m)?
K-19A	199 ± 1	776 ± 2	1.00	280	P-1	Phl + Qtz
K-19B	199 ± 1	776 ± 2	1.00	280	K-10	Phl + Qtz + En(tr)
K-10	200 ± 1	800 ± 1	1.00	263	P-1	Phl + Qtz + En(m) + Gl(m)?
K-11	200 ± 1	812 ± 4	1.00	242	P-1	Phl + Qtz + En + Gl(m)
K-118	504 ± 4	807 ± 16	1.00	215	P-1	Phl + Qtz
K-103	506 ± 1	809 ± 1	1.00	161	P-1	Phl + Qtz
K-115	503 ± 1	836 ± 2	1.00	118	P-1	Phl(m) + En + Gl
K-76	1007 ± 25	740 ± 1	1.00	119	P-1	Phl + Qtz
K-78	1003 ± 24	750 ± 1	1.00	111	P-1	Phl + Qtz
K-74	1010 ± 33	760 ± 1	1.00	122	P-1	Phl + Qtz + En + Gl
K-68	996 ± 36	765 ± 1	1.00	122	P-1	Phl + Qtz + En + Gl
K-67	1001 ± 37	770 ± 1	1.00	96	P-1	Phl + Qtz + En(m) + Gl(m)?
K-42	1000 ± 22	775 ± 1	1.00	85	P-1	Phl + Qtz + En(tr)
K-5	1010 ± 20	780 ± 1	1.00	159	P-1	Phl + Qtz + En(m) + Gl(m)
K-77	1524 ± 21	785 ± 1	1.00	47	P-1	Phl + Qtz + En + Gl(m)
			Reaction (Fl)			
K-113	502 ± 3	855 ± 1	dry	167	P-1	Phl(m) + Qtz + En + Sa(m)
			Reaction (Qtz)			
K-20	51.0 ± 0.3	860 ± 2	1.00	240	P-5	En + Sa
K-110	52.4 ± 0.7	949 ± 4	1.00	124	P-5	En + Sa
K-14	101 ± 1	950 ± 15	1.00	168	P-5	Phl + En(m) + Gl

* In parentheses, m = minor amount of phase, tr = trace amount of phase.

ple locations in the vessels. Pressure was monitored using a solid-state transducer accurate to ±0.6 MPa. Week-long experiments at 100 MPa and 800 °C, with Pt capsules containing various metal-oxide-H_2O systems, showed that the intrinsic f_{O_2}/f_{H_2} of the system was close to $Fe_3O_4 + Fe_2O_3 + H_2O$ or $Cu + Cu_2O + H_2O$.

One high-temperature experiment on (Qtz) (950 °C, 100 MPa) was performed in a large-volume, internally heated pressure vessel at Clermont-Ferrand. N_2 was the pressure medium and the vessel was operated with the long axis of the furnace horizontal. The vertical thermal gradient was measured by two type-B (PtRh6%-PtRh30%) thermocouples, one on either side of the sample. Temperatures are believed accurate to ±2 °C. Pressure was measured from the output of a manganin cell, itself calibrated against a Bourdon tube gauge.

Experiments at 500 MPa. One 500 MPa experiment used a large-volume, internally heated vessel in the Department of Earth Sciences at Monash University, Australia. The vessel was held vertically and is similar to that described by Burnham (1962). The pressure medium was Ar, and the samples were heated by two-zone, inconel, resistance furnaces. Pressure was measured by a manganin resistance cell, itself calibrated against a 0–700 MPa Heise gauge. Temperatures were monitored with type-K thermocouples calibrated against a type-S standard thermocouple (itself calibrated by the National Measurement Laboratory, C.S.I.R.O., New South Wales, Australia). The reported temperature is accurate to ±2 °C. In the experiment, f_{H_2} was imposed by a H diffusion membrane of $Pd_{60}Ag_{40}$. O_2 fugacity was 1.3 (±1) log units below FMQ, as calibrated by O'Neill (1987). The rest of the 5 kbar experiments used small-volume, internally heated Ar vessels at Arizona State University and in Manchester University. The vessels were held horizontally, with single-zone furnaces. Pressures were measured by manganin cells and temperatures by two type-K thermocouples. Pressure and temperature uncertainties are similar to those quoted for the large-volume vessels.

Experiments at $P \geq 1.0$ GPa. All higher-pressure experiments were performed in small, non-end-loaded, 1.27 cm, piston-cylinder apparatus (Patera and Holloway, 1982) at Manchester and Clermont-Ferrand. Pressure cells were all NaCl with graphite furnace tubes. Temperatures were measured with WRe_5-WRe_{26} thermocouples, calibrated against the 1.0 GPa melting point of Au (1120 °C;

Akella and Kennedy, 1971), or with type-R thermocouples. Thermal gradients of ~2 °C across the 0.6 mm thick samples are estimated from the measurements of Esperança and Holloway (1986) and Jakobsson and Holloway (1986) on this type of sample assembly. Reported temperatures are considered accurate to ±2 °C.

Starting materials

Phlogopite. The pure, synthetic hydroxyphlogopite used in this study is the same material used by Vielzeuf and Clemens (1992). The reader is referred to this earlier work for details on its synthesis and characterization. None of the phlogopite starting material was analyzed directly. However, some analyses of recrystallized phlogopite from subsolidus experiments are presented later.

Sanidine. The sanidine was crystallized from a gel made according to the method of Hamilton and Henderson (1968). A small amount of the powdered gel was fused and quenched to a glass on an Ir-strip heater (Nicholls, 1974). Electron probe analysis gave the following composition in weight percent: SiO_2 = 65.52(74), Al_2O_3 = 18.81(18), MgO = 0.11(18), CaO = 0.03(10), Na_2O = 0.00, and K_2O = 16.16(72), where the figures in parentheses are 2σ uncertainties. Note that the measured MgO and CaO contents are lower that the uncertainties; they thus have effectively zero concentrations, being at or below detection limit. The gel was crystallized with excess H_2O at 360 MPa and 700 °C for 300 h. Optical and powder X-ray examination revealed only the presence of pure, high sanidine; the structural state was checked by the method of Wright (1968).

Enstatite. The enstatite was synthesized from a gel plus excess H_2O at 200 MPa and 800 °C for a total of 284 h. After the first 121 h, the product contained much unreacted gel but, after being reground and heated for a further 163 h, optical examination showed only pure orthoenstatite. This was confirmed by X-ray powder diffractometry, which yielded the following cell dimensions: a = 18.220(36), b = 8.814(8), and c = 5.157(5) Å, with 2σ uncertainties. In my experience, oxide mixes react more rapidly in the synthesis of pyroxenes, and so I recommend that gels not be used.

Quartz. All quartz used in these experiments was finely ground (−10 μm), acid washed, Brazilian, optical grade, rock crystal.

Chemical reagents. Analytical-grade K_2CO_3, Al metal powder, and MgO were used in the synthesis of phlogopite, sanidine, and enstatite. The K_2CO_3 was dried at 110 °C and the MgO fired at 1200 °C; both were stored in a vacuum desiccator until use. The tetraethyl orthosilicate (TEOS) used as a source of SiO_2 in the sanidine gel was standardized in triplicate to give 28.686 ± 0.034 wt% SiO_2. Distilled, deionized H_2O was used in all cases.

Starting mineral mixtures. Three different mineral mixtures were used as starting materials. P-1 is a phlogopite + quartz mixture (1:1 by weight), P-3 is a quartz + sanidine + phlogopite mixture (4.55:4.55:1 by weight), and P-5 is an enstatite + sanidine mixture (3.5:6.5 by weight); these are plotted in Figure 2. The P-1 and P-3 mixtures were made by grinding the pure, synthetic minerals (plus quartz) together, in an agate mortar, under acetone, for 20 min. Mixture P-5 was made by gentle hand grinding in the agate mortar, so as to avoid quartz contamination. All mixes were dried at 110 °C and stored in vacuum desiccators over silica gel.

Experimental techniques

For experiments at $P \leq 200$ MPa, thin-walled Pt capsules were loaded with about 0.02 g of starting material. In H_2O-saturated experiments, water was measured into the capsule by microsyringe. The water was weighed and the capsules sealed by carbon arc welding.

For 500 MPa experiments, the capsules were $Pd_{50}Ag_{50}$ or $Pd_{30}Ag_{70}$ and sample masses were 0.015–0.02 g. Water was added prior to closure. In the experiments at higher P, approximately 0.02 g of starting material were loaded into small Pt capsules. About 0.005 g of water was added before welding. In all cases, the capsules were then squashed flat and folded into packets with approximate dimensions of 3.5 × 5 × 0.6 mm. These packets were laid flat in the pressure cells so that the samples would experience minimal thermal gradients.

All experiments were simultaneously brought to final P-T conditions. Samples were initially pressurized to near final experimental P, and the furnace was then switched on. Expansion of the heating sample increased P, and this was continuously lowered to maintain the final desired experimental P. Thus, the hot piston-out technique was used. In most cases, the experimental P was kept constant using a hydraulic screw press actuated by alarm relays from a digital pressure meter. Experimental conditions were monitored and recorded several times per day over the course of each experiment. Reported temperatures are the averages of the minimum and maximum recorded, and quoted uncertainties represent the total ranges of temperature variation during the experiments. A similar procedure was followed for the pressure measurements. To avoid vesiculation of volatile-bearing glasses, all experiments were quenched isobarically. Quench rates were ~100 °C/s in the piston cylinders, 3 °C/s in the cold-seal vessels (cooled by air jet), and 1 °C/s in the internally heated vessels.

After the experiments, survival of the capsules was checked by comparing post- and preexperiment masses. The results for any capsule showing a significant mass loss (>0.0005 g) would have been disregarded. None of the capsules ruptured during successfully stabilized experiments.

Observation and analysis of experimental products

The contents of each capsule were split into several portions. Part was ground under acetone and used to make an optical grain mount in oil with R.I. = 1.536. Microscopic examination of these grain mounts was the principal method of phase identification. In some cases, though not identifiable in grain mount, the presence of glass was

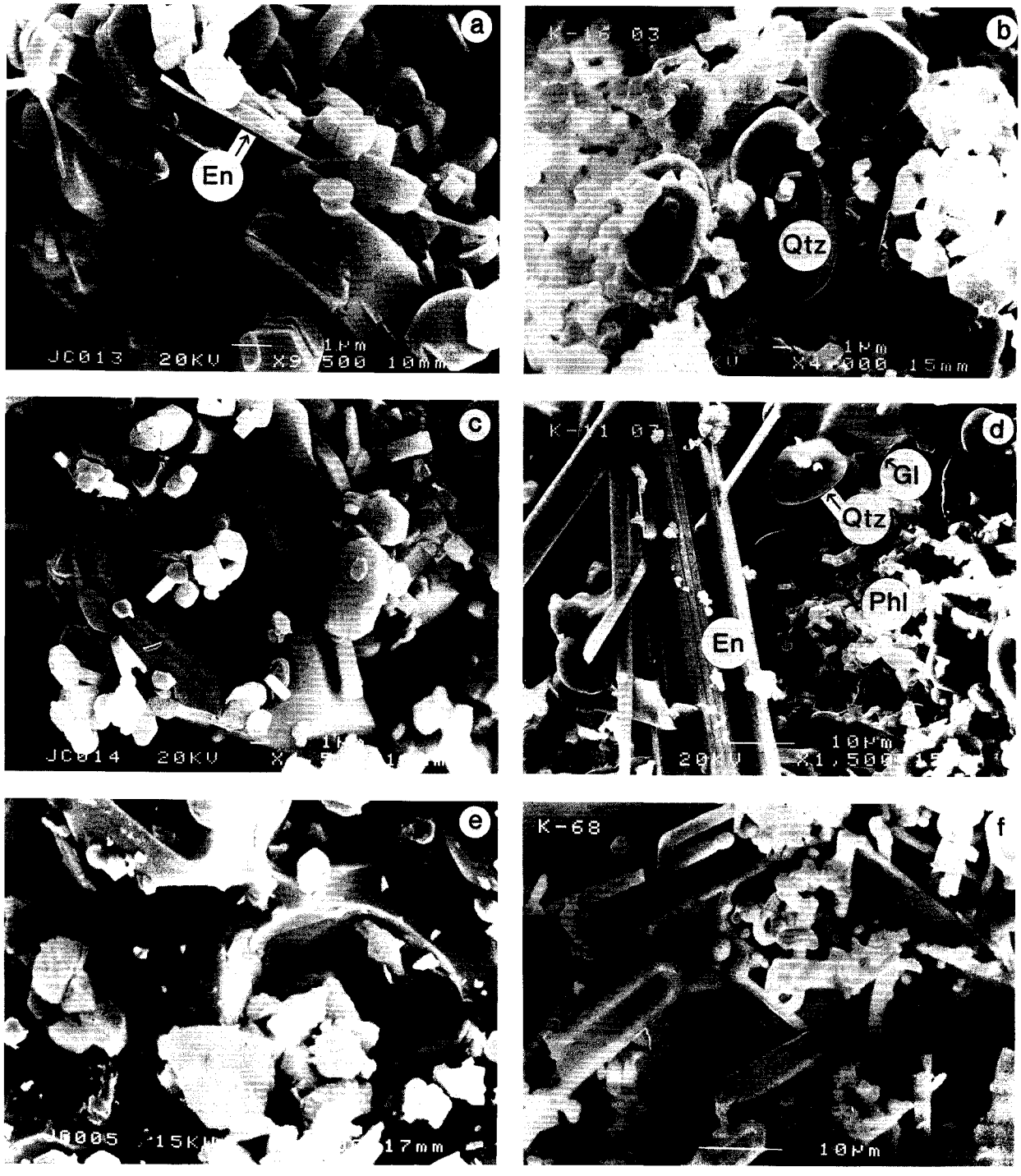

inferred from the coherence and brittleness of the sample when crushed; unmelted samples are soft powders. X-ray diffraction techniques were used for the detection of sanidine because optical identification proved difficult.

CGR, Phillips, and Siemens type-F diffractometers were used for the powder X-ray work. Cu$K\alpha$ radiation was used and 2θ-D relations were calibrated against Au and quartz internal standards. Samples were finely ground under acetone and sedimented onto glass slides. SEM and electron probe examination used the Manchester University JEOL JSM 6400 fitted with a Link EXL EDS analytical system and an Oxford Instruments cryo-stage. ZAF4 software was used for data processing. For SEM examination, experimental products were lightly crushed,

Fig. 4. SEM, secondary electron photomicrographs of selected experimental products. (a) Phlogopite booklets and some very thin enstatite needles (En) formed in subsolidus expt. K-23 on reaction (M) (51 MPa, 800 °C, 383 h). (b) Recrystallized quartz (Qtz) and phlogopite platelets from expt. K-16 on reaction (Sa) (199 MPa, 286 °C, 280 h), in which no reaction occurred. (c) Recrystallized quartz and phlogopite booklets in expt. K-19A on reaction (Sa) (199 MPa, 776 °C, 280 h). Only a trace of enstatite formed and none is present in this view. (d) Large enstatite needles (En), glass = quenched melt (Gl), recrystallized quartz (Qtz), and residual phlogopite platelets (Phl) in expt. K-11 on reaction (Sa) (200 MPa, 812 °C, 242 h). The extent of reaction here is only a little greater than in K-19A (in c), yet the products (En and Gl) are far more prominent. (e) Glass (quenched melt) formed in expt. K-42 on (Sa) (1 GPa, 775 °C, 85 h). Note the rounded anhedral quartz crystals embedded in the glass and pits left where these have been plucked out. (f) Expt. K-68 on (Sa) (996 MPa, 765 °C, 122 h), which was just above the solidus. Here phlogopite platelets are decorated with spheroids and pipings of highly siliceous, fluid-phase quench glass.

←

mounted on Al stubs with double-sided adhesive tape, and coated with Au using a sputter coater. All analyses were performed on polished sections of experimental products set in drops of epoxy resin on glass slides. The reader is referred to Vielzeuf and Clemens (1992) for further details on the use of the cryo-stage for the analysis of quench glasses.

Identification and description of phases in experimental products

For the congruent melting reactions (En) and (Phl) and for reaction (Qtz), there is no difficulty in detecting the onset of reaction. When melting occurs by these reactions, large proportions of glass appear in the experimental products. In contrast, subsolidus reaction (M) and incongruent melting reaction (Sa) both involve the breakdown of phlogopite to produce enstatite and sanidine or melt, respectively. As with the fluid-absent reaction (see Vielzeuf and Clemens, 1992), these are far more sluggish, producing only tiny proportions of the product phases when within 10 °C or so of the phase boundary, especially at pressures of 200 MPa or less. Thus, it was important to examine the experimental products with the SEM to detect the first appearance of enstatite, the best indicator of reaction as T increases.

Phlogopite. Phlogopite mostly forms very fine-grained felted masses in which individual crystals are difficult to distinguish without the SEM. However, there are usually a few crystals that attain a respectable size (≤ 10 μm). These larger grains are colorless and have medium relief (which varies with crystal orientation), high birefringence, and straight extinction. Some examples are shown in Figure 4 and some analyses are given in Table 3.

Quartz. This phase always forms rounded grains with low relief and low birefringence. In fluid-present and all super-solidus experiments, quartz grains are commonly larger (≤ 25 μm) than in the starting material. The larger crystals have rounded, subhedral β habits (see e.g., Fig. 4c).

Enstatite. Orthoenstatite formed high-relief needles and prisms with straight extinction and very low birefringence. The forms of enstatite crystals vary dramatically as a function of several factors. They were generally much smaller in low-P experiments and experiments without significant quantities of glass (quenched melt). Very elongate, needle-like crystals are the general rule (length-width ratio averaging about 8). In experiments on (Sa) at 1.0 GPa, these needles attain lengths of up to 1 mm. At low pressures (≤ 200 MPa), a fraction of the crystals usually have markedly inclined extinction, indicating some metastable formation of clinoenstatite. See Figure 4a and 4d for examples and Table 3 for some analyses.

Glass (quenched melt). Glass, when present in sufficient

TABLE 3. Averages and number of analyses (n) and structural formulae of crystalline phases

	Subsolidus expts.		Supersolidus expts.				
Expt.	K-2	K-78	K-9	K-11	K-11	K-115	K-115
P (MPa)	101	1003	200	200		503	
T (°C)	769	750	791	812		836	
Phase	Phl	Phl	Phl	Phl	En	Phl	En
n	3	5	2	2	2	5	3
SiO_2	44.47(0.90)	43.91(1.13)	44.31(0.36)	45.65(0.42)	61.33(1.78)	45.16(1.05)	61.21(0.72)
Al_2O_3	12.26(0.28)	11.75(0.49)	11.95(0.06)	11.83(0.01)	n.d.	11.87(0.48)	0.12(0.20)
MgO	28.11(0.76)	27.36(0.77)	28.25(0.19)	26.17(0.19)	39.69(1.00)	26.83(1.12)	38.52(0.48)
K_2O	10.99(0.08)	10.47(0.32)	10.33(0.24)	10.49(0.26)	n.d.	11.47(0.49)	n.d.
Total	95.83(1.88)	93.49(2.49)	94.84(0.47)	94.15(0.02)	101.02(2.78)	95.33(2.56)	99.84(1.37)
O^{2-}	11	11	11	11	3	11	3
Si	3.067	3.095	3.076	3.180	1.012	3.132	1.020
Al	0.996	0.976	0.978	0.970		0.970	0.002
Mg	2.889	2.875	2.923	2.717	0.976	2.773	0.957
K	0.967	0.941	0.915	0.932		1.015	

Note: n.d. = not detected; 1σ values given in parentheses.

TABLE 4. Normalized analyses (100% anhydrous means of *n* analyses) of glasses (quenched melts)

Reaction	(En)	(En)	(En)	(Sa)	(Sa)	(Sa)	*	*
Data source	1	1	2	2	2	1	3	3
Expt.			K-107	K-11	K-115			
P (MPa)	200	1000	1499	200	503	1000	300	700
T (°C)	760	722	725	812	836	830	702	690
n	6	6	3	1	3	4	?	?
SiO_2	81.87(1.75)**	79.84(0.71)	77.64(0.09)	82.94	81.67(0.07)	82.98(1.17)	74.38	74.07
Al_2O_3	10.67(0.19)	12.19(0.12)	11.6(0.12)	8.92	9.25(0.06)	10.59(0.24)	14.27	14.51
FeO†	n.a.	n.a.	n.d.	n.a.	n.d.	n.a.	1.25	1.30
MgO	0.12(0.03)	0.18(0.03)	0.09(0.13)	0.38	0.35(0.03)	0.65(0.04)	0.30	0.28
Na_2O	n.a.	n.a.	n.d.	n.a.	n.d.	n.a.	5.60	5.94
K_2O	7.34(0.95)	7.79(0.69)	10.66(0.45)	7.77	8.74(0.09)	5.78(1.02)	4.19	3.90
Original total	92.74(1.24)	89.64(0.41)	90.71(1.35)	93.01	90.82(0.94)	89.91(1.01)		

Note: data source 1 = Peterson and Newton (1989), 2 = present work, and 3 = Hoffer and Grant (1980); n.d. = not detected; n.a. = not analyzed.
* Low-*T* melting reaction in Na- and Fe-bearing system.
** 1s values given in parentheses.
† Total Fe as FeO.

quantity, was obvious in grain mounts. It forms colorless, isotropic masses with high relief and $n <$ oil. In experiments at $P \geq 500$ MPa, colorless, isotropic glass formed easily recognizable patches, interstitial to enstatite crystals in the case of reaction (Sa); see Figure 4e. At lower pressures, near the solidus, glass was not readily identifiable by optical means. Its presence was inferred from the brittleness and hardness of the experimental products when they were being crushed in an agate mortar and verified by SEM examination (e.g., Fig. 4d). In some cases, powder XRD patterns also showed a glass hump. This problem results from the small extents of reaction owing to the extreme sluggishness of phlogopite breakdown at $P < 500$ MPa and $T < 800$ °C. Table 4 shows the compositions of some glasses formed in the experiments on (En) and (Sa). In some experiments, just above the solidus at 1 GPa, where only small amounts of melt formed, it was also possible to identify a glass formed by fluid-phase quenching. This material forms tiny spheroidal beads or piping that decorates the margins of residual phlogopite platelets (see Fig. 4f). This phase is distinguished from the quenched melt by its lower refractive index (higher negative relief in oil), its form, and its composition (nearly pure silica on qualitative EDS analysis).

RESULTS OF THE PRESENT WORK

Table 2 shows the conditions of each experiment and the phases identified in the experimental products. Table 3 shows some analyses of the crystalline phases in the experimental products, and Table 4 shows the analyses of the glasses (quenched melts).

Locations of reactions in *P-T* space

For reaction (M), the results of six experiments, at pressures below 100 MPa, agree with the data of Wones and Dodge (1977) and Wood (1976). As a consequence of the very tight constraints these place on the locus of the reaction, it is possible to refine the value for the free energy of formation of Al-Si–disordered phlogopite, reducing the uncertainty on the calorimetrically determined value (Clemens et al., 1987) by 46%. The new value for ΔG_f°Phl (-5838.16 ± 3.37 kJ/mol) was calculated assuming that S°, V°, the C_P equation, thermal expansivity, and compressibility of phlogopite, and that the thermodynamic properties for all other phases participating in the reaction (as used in Clemens et al., 1987) are correct, and adjusting ΔG_f°Phl within the limits imposed by the calorimetric results. The new value facilitates far more tightly constrained and useful thermodynamic calculations of equilibria involving this mineral.

Constraints obtained from the four experiments on reaction (En), as well as the data from earlier workers (see Table 1), indicate that the reaction is almost coincident with Sa + Qtz + Fl = M in the MgO-free analogue system. This is confirmed by the melt compositions (see below) and means that the relatively well-known solidus in the MgO-free system can be confidently used to interpolate between and extrapolate beyond the limits of the rather few points on (En) and (Phl).

For reaction (Sa), 18 experiments were performed at pressures ranging from 200 MPa to 1.5 GPa. The reaction was tightly bracketed at 200 MPa, 500 MPa, and 1 GPa, and reversed at 200 MPa. Work at 1.5 GPa was limited to a single experiment (K-77), which provides an upper temperature limit and complements the low-*T* half-bracket obtained by Peterson and Newton (1989). Contrary to the prediction of Wones and Dodge (1977) and the reported results of Bohlen et al. (1983), reactions (Sa) and (En) are nowhere near being coincident. I can provide no cogent explanation for the apparent discrepancy between Bohlen et al. (1983) and other results. However, reaction (Sa) lies approximately 95 °C above reaction (En) at 500 MPa. In agreement with the present results, a difference of about 60 °C was reported by Peterson and Newton (1987, 1988) at 1.5 GPa. However, the present results imply that the difference is <20 °C at 200 MPa. Thus, as shown in Figure 3, reaction (Sa) would appear to exhibit graceful swings form positive to negative d*P*/

dT slopes at pressures up to 1 GPa. At higher P, the slope probably remains positive. These slope changes are well constrained by the data.

In Figure 3, it is apparent that the slope changes in reaction (Sa) vary in sympathy with those determined by Vielzeuf and Clemens (1992) for (Fl). Because the data for the two reactions were obtained at different times, by different workers, in different laboratories, using different apparatus, this parallelism cannot be dismissed as an experimental artifact. It must reflect a complex interplay of thermochemical parameters for the common phases involved (Phl, Qtz, En, and M). Vielzeuf and Montel (1994) noted similar slope changes in phase boundaries involving biotite breakdown in a metagraywacke. Perhaps the most important factor is the balance between the molar volumes and entropies of the solid phases and those of the hydrous melt. The ultimate controls are probably subtle variations, with pressure, of the partial molar volume and entropy of H_2O in the hydrous aluminosilicate melt.

The single new experiment on (Fl), at 502 MPa, confirms Vielzeuf and Clemens's (1992) location of this equilibrium and shows that sanidine is unequivocally a product phase over the entire pressure range investigated.

The three experiments on (Qtz), together with previous data, and the preferred location of the invariant point I_1 at 807 °C and 58 MPa suggest a slightly negative slope for the reaction. According to all the compiled data, (Qtz) could have either a positive or a slightly negative slope. There are no tight experimental constraints on the position of the high-T invariant point at which phlogopite, sanidine, enstatite, forsterite, melt, and fluid coexist, and where (Qtz) terminates. The data of Luth (1967) constrain it to lie at some pressure between 41 and 69 MPa and a temperature <1000 °C. This is compatible with either a slightly positive or a slightly negative slope. It appears that the reaction is almost flat in P-T space. However, a negative dP/dT slope would place the melt phase on the high-T side, which seems more logical than previous depictions with melt on the low-T side.

Univariant or divariant?

An issue of some importance is whether the equilibria dealt with here are univariant or divariant. Divariance could be caused by mineral phases involved in the equilibria changing their stoichiometry so as to depart from their ideal formulae.

In the present context, the only phases for which this is a significant possibility are phlogopite and enstatite. Micas are notorious for their development of complex solid solutions involving many sorts of cationic, anionic, and vacancy substitutions, many of them coupled. Though rather simple, phlogopitic micas in the present system are capable of showing many such phenomena. The main possibilities are vacancy substitution (K deficiency) in the interlayer site coupled with $^{[6]}$Al substitution (wonesite solid solution), and Al substitution for $^{[6]}$Mg coupled with $^{[4]}$Al substitution for Si (eastonite solid solution) (see Bailey, 1984, and references therein). The hallmark of both of these substitutions is that the mica is more aluminous than stoichiometric phlogopite. Enstatite could depart from stoichiometry, becoming aluminous through the coupled substitution of $^{[6]}$Al and $^{[4]}$Al for Mg and Si, respectively. Peterson and Newton (1987, 1988, 1989) suggested that they could identify slight divariant character in the various melting equilibria, caused by the peraluminous nature of their starting phlogopite.

There is no suggestion of a detectable divariant interval in the data for phlogopite breakdown by subsolidus reaction (M). Thus, if any of the melting equilibria are divariant, the thermal interval must also be very narrow, especially at low P.

The compositions of phlogopite grown in both subsolidus and supersolidus experiments are shown in Table 3. The quality of the analyses is somewhat impaired by the relatively poor state of polish on the tiny mica flakes and the great difficulty of obtaining analyses free from influence by surrounding phases. However, there is no evidence in these analyses suggesting that the micas are peraluminous. The phlogopite produced below the solidus (recrystallized starting micas) is essentially the same as that grown in the presence of melt. The enstatite is not aluminous either. Thus, there is no clear evidence here for divariant character in (Sa).

Phlogopite persists in many experimental products that produced melt through reactions (Sa) and (Fl) (see Table 2; see also Table 1 of Vielzeuf and Clemens 1992). This could be ascribed to the occurrence of a divariant interval for these reactions. However, sluggish reaction kinetics have been observed by all experimental groups working in this magnesian system. Thus, slow reaction rates are a credible explanation for this persistence of phlogopite. The maximum extent of any divariant interval is constrained to be 27 °C by the present experiments.

Phlogopite coexistence with melt at temperatures above congruent reaction (En), but below (Sa), only implies that the experiments were conducted in such a way that phlogopite was in excess of that required to saturate the melt. No divariance is implied here.

In summary, though it is possible that some small degree of divariance exists for (Sa) and (Fl), the evidence suggests that the equilibria can be treated as essentially univariant in this simple system. Analogue reactions for natural complex biotite are, of course, polyvariant; melting intervals are well established in such cases (e.g., Vielzeuf and Montel, 1994).

Melt compositions

Table 4 shows the compositions of glasses (quenched melts) obtained in the present work. Also shown are analyses of glasses from previous studies, including some of the melting reaction Bt + Nafs + Qtz + Fl = Opx + M in the more complex system $KAlO_2$-$NaAlO_2$-FeO-MgO-SiO_2-H_2O (Hoffer and Grant, 1980), where the mica had Mg/(Mg + Fe) = 0.5. Nafs symbolizes Na-rich alkali feldspar, and Opx symbolizes a complex orthopyroxene solid solution. The original probe totals are around 91 wt%.

This is a typical value for hydrous glasses rich in low atomic number elements and indicates good analytical quality.

Note that in Table 4, the MgO contents of the melts are very low. The low solubility of MgO in these H_2O-saturated siliceous (granitoid) melts agrees with results on the fluid-absent reaction in the system (Vielzeuf and Clemens, 1992). Thus, although reactions (En) and (Phl) must lie at lower T than Sa + Qtz + Fl = M, the amount of solidus depression due to the presence of MgO must be rather small.

There is a weak, positive, linear correlation ($r^2 = 0.682$) between the MgO contents of quench glasses formed by the fluid-present melting reactions (En) and (Sa) and experimental T. Intriguingly, the same concentration data show a strong linear correlation ($r^2 = 0.929$) with ΔT, the number of degrees celsius by which the experiment exceeded the solidus T of the particular reaction (i.e., the degree of thermal overshoot). This correlation is not induced through the mathematical manipulation of the data. Thus, although MgO solubility increases with T, a stronger control seems to be the degree of thermal overshoot above the melting reaction. This is curious and implies that there may be some feedback mechanism operating, in which the melt-crystal system is thermodynamically aware of the overshoot and the absolute experimental T.

Melt proportions

H_2O contents of melts formed by (Sa) and (Fl) were calculated for pressures up to 1 GPa using the solubility model of Burnham (1979) and Burnham and Nekvasil (1986). The low MgO solubility in the melts permits use of the Sa-Qtz-H_2O system as a model, with the silicate portion of the melt assumed to have a constant composition of 60 wt% Sa and 40 wt% Qtz. At any pressure along the equilibrium curve for (Fl), the a_{H_2O} was calculated using the computer program of Nekvasil and Burnham (1987); see also Figure 7 of Vielzeuf and Clemens (1992). From these melt H_2O contents, it is possible to calculate the proportions of melt formed by breakdown of a phlogopite + quartz mixture (1:1 weight ratio) by the two equilibria, assuming that H_2O is in excess, in the case of reaction (Sa). At very low pressures, fluid-absent melting can yield as much melt as the fluid-present reaction but, at 1 GPa, only a little over half as much. For the fluid-present reaction, there is only very modest increase in melt proportion as P increases. This is because the relatively small increase in H_2O content of the melt, as P rises, is the only factor affecting melt proportion.

For natural quartzofeldspathic rocks this means that fluid-present reactions may produce large amounts of melt, almost independent of pressure. Under H_2O-saturated conditions, this could form migmatites with large melt fractions, depending on the quartz-feldspar ratios. The ultimate limit is probably the availability of aqueous fluid. In contrast, fluid-absent melt proportions are commonly far lower for a given source rock (e.g., Clemens and Vielzeuf, 1987; Johannes and Holtz, 1990). With these gross differences in melt volumes, the physical behavior of partially molten crust is likely to have a strong dependence on the type of melting reaction (see Brown et al., 1995).

Melt mobility in the crust

If (Fl) is taken as a model for fluid-absent biotite breakdown in quartzofeldspathic rocks and metagraywackes at granulite grade, it is clear from the constant positive or infinite dP/dT slope of the equilibrium (Fig. 3), that adiabatic ascent of the melt to very high crustal levels is possible. This is in agreement with the inferred origin of many granitoid batholiths and silicic volcanic complexes (e.g., Fyfe, 1973; White and Chappell, 1977; Clemens and Wall, 1981; Clemens, 1990; Thompson, 1990; Vielzeuf et al., 1990; Brown, 1994).

On the other hand, many migmatites seem to have been formed through fluid-saturated partial melting reactions in the amphibolite-facies middle crust (e.g., Clemens and Wall, 1981; Clemens, 1990; Thompson, 1990; Brown, 1994). If this melting occurred by reactions similar to (Sa), the negative dP/dT slopes of such reactions would seem effectively to prohibit magma ascent. Freezing would occur if the magma attempted ascent, regardless of the P-T path followed. However, if the natural reactions exhibit slope changes similar to that of (Sa), it may be possible for some H_2O-saturated melts formed by biotite breakdown to ascend significant distances without crossing their solidus. For (Sa) this would occur only at pressures of 250–500 MPa (Fig. 3). However, it is very unlikely that free, pervasive aqueous fluid would be present at pressures of 1 GPa or greater.

Biotite stability in wet granitic magmas and migmatites

At pressures between 100 and 500 MPa, phlogopite is stable in the presence of H_2O-saturated granitoid (silica-rich) melt to around 800 °C (see Fig. 3). In H_2O-saturated natural rock (granite to granodiorite) experiments (e.g., Piwinskii, 1968, 1973a, 1973b; Piwinskii and Wyllie, 1968; Maaløe and Wyllie, 1975; Clemens and Wall, 1981), biotite is stable to around 810–860 °C. Thus, natural biotite seems to be more thermally stable. As with the fluid-absent reaction (Vielzeuf and Clemens, 1992), (Sa) seems to be a reasonable model for the stability of some natural biotites in partial melting and crystallization of quartz-saturated metaluminous systems. The enhanced stability of the natural micas is probably due to the presence of additional components such as F and Ti (see e.g., Forbes and Fowler, 1974; Munoz and Ludington, 1974; Robert, 1976; Tronnes et al., 1985; Peterson et al., 1991, and Patiño Douce, 1993).

A potential equilibrium problem

The equilibria depicted in Figure 3 can all be experimentally bracketed and reversed. However, this does not prove that they are stable. It is possible to perform experiments on metastable equilibria without ever encountering the stable ones provided that there is a sufficiently strong kinetic barrier to the crystallization of at least one of the stable phases.

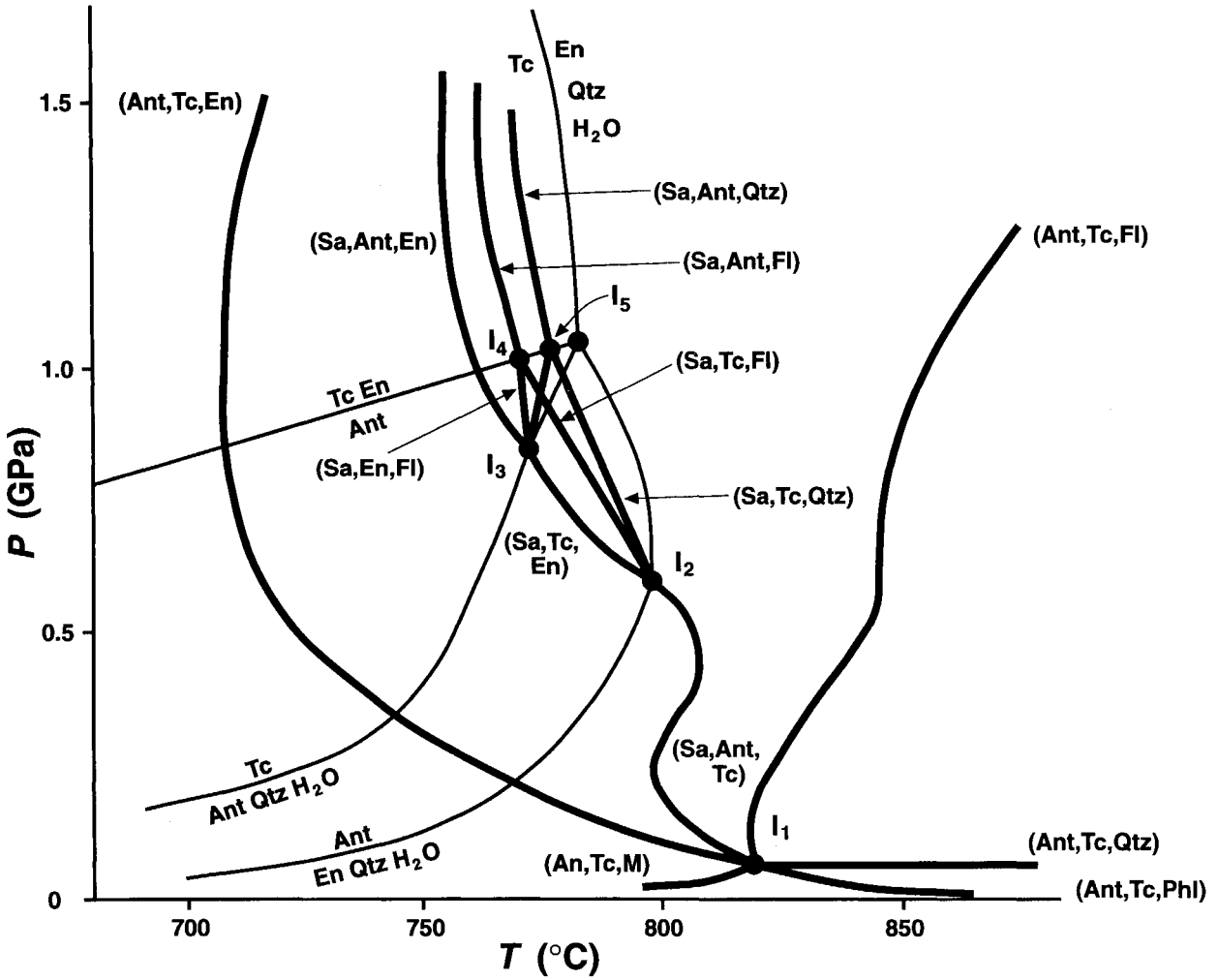

Fig. 5. *P-T* sketch plot of the theoretical reaction bundles that could be created by the effects of the talc and anthophyllite equilibria on the phase relations shown in Fig. 3. The equilibria shown as thin lines are the relations among the phases Tc, Ant, En, Qtz, and H_2O in the system $MgO\text{-}SiO_2\text{-}H_2O$; the invariant point is marked by the unlabeled dot. Thick lines are the equilibria in the larger system (with $KAlO_2$) and are labeled according to the three absent phases in each case. The invariant points (labeled dots) are numbered, as in the text.

Existing experimental and thermodynamic constraints suggest that the anthophyllite dehydration reaction (Ant = 7En + Qtz + H_2O) intersects reaction (Sa) at some pressure between 600 and 700 MPa (Fig. 5). This would form a new invariant point (I_2), render (Sa) metastable, and introduce the following new equilibria into the system (Fig. 5):

$$\text{Phl} + \text{Qtz} + \text{Fl} = \text{Ant} + \text{M} \quad \text{(Sa, Tc, En)}$$

$$\text{Phl} + \text{Ant} + \text{Qtz} = \text{En} + \text{M} \quad \text{(Sa, Tc, Fl)}$$

$$\text{Phl} + \text{Ant} + \text{Fl} = \text{En} + \text{M} \quad \text{(Sa, Tc, Qtz).}$$

Likewise, the talc dehydration reaction (7Tc = 3Ant + 4Qtz + $4H_2O$) would appear likely to intersect reaction (Sa, Tc, En) (depending upon its slope) at some pressure above 800 MPa. If this occurs, the following equilibria would sprout from yet another invariant point, I_3 (Fig. 5):

$$\text{Phl} + \text{Qtz} + \text{Fl} = \text{Tc} + \text{M} \quad \text{(Sa, Ant, En)}$$

$$\text{Phl} + \text{Tc} + \text{Qtz} = \text{Ant} + \text{M} \quad \text{(Sa, En, Fl)}$$

$$\text{Phl} + \text{Tc} + \text{Fl} = \text{Ant} + \text{M} \quad \text{(Sa, En, Qtz).}$$

At still higher pressures (above 1 GPa), where anthophyllite is no longer stable, there must be a further invariant point (I_4). Here, reactions (Sa, En, Fl) and (Sa, Tc, Fl) terminate and are replaced by the equilibrium (Fig. 5) Phl + Tc + Qtz = En + M (Sa, Ant, Fl), and at I_5 the Qtz-absent reactions are replaced by Phl + Tc + Fl = En + M (Sa, Ant, Qtz).

Though they are likely to be stable, none of the melting equilibria involving anthophyllite have ever been encountered experimentally. This is almost certainly a con-

sequence of the huge kinetic barrier to the crystallization of this phase, as noted by Greenwood (1963). Indeed, anthophyllite crystallization in natural rocks (e.g., Droop, 1994) and in laboratory synthesis (e.g., Chernosky et al., 1985) is severely hampered by the formation of triple-chain pyriboles. Given this problem, it may be impossible to determine experimentally the stable *P-T* phase diagram at pressures above about 500 MPa.

Acknowledgments

Most experiments for this work were performed at Manchester University, with support from NERC grant GR3/7669. Some of the lower-pressure and a few piston-cylinder experiments were done at Clermont-Ferrand, while the author was visiting as Directeur de Recherche Associé. One gas-vessel experiment was performed while the author was visiting John Holloway's laboratory at Arizona State University. Unit-cell parameters for the synthetic phlogopite and enstatite were determined by Yves Blanc at Clermont-Ferrand, Jacques Kornprobst and Pierre Boivin assisted with the Clermont internally heated pressure vessel. Daniel Vielzeuf helped with the initial analysis of the effects of anthophyllite stability in the system. I am grateful to all these organizations and individuals for the help that they provided. Thorough and critical reviews by Jon Peterson and an anonymous reviewer greatly improved the clarity of the paper.

References cited

Akella, J., and Kennedy, G.C. (1971) Melting of gold, silver, and copper: Proposal for a new high-pressure calibration scale. Journal of Geophysical Research, 76, 4969–4977.

Bailey, S.W. (1984) Crystal chemistry of the true micas. Mineralogical Society of America Reviews in Mineralogy, 13, 13–60.

Bohlen, S.R., and Boettcher, A.L. (1982) The quartz ↔ coesite transformation: A precise determination and the effects of other components. Journal of Geophysical Research, 87, 7073–7078.

Bohlen, S.R., Boettcher, A.L., Wall, V.J., and Clemens, J.D. (1983) Stability of phlogopite-quartz and sanidine-quartz: A model for melting in the lower crust. Contributions to Mineralogy and Petrology, 83, 270–277.

Brown, M. (1994) The generation, segregation, ascent and emplacement of granite magma: The migmatite-to-crustally-derived granite connection in thickened orogens. Earth-Science Reviews, 36, 83–130.

Brown, M., Rushmer, T., and Sawyer, E.W. (1995) Mechanisms and consequences of melt segregation from crustal protoliths. Journal of Geophysical Research, in press.

Burnham, C.W. (1962) Large volume apparatus for hydrothermal investigations to 10,000 bars and 1500 °C (abs.). American Ceramic Society Program, Seattle, Washington.

——— (1979) The importance of volatile constituents. In H.S. Yoder, Ed., The evolution of the igneous rocks (Fiftieth Anniversary Perspectives), p. 439–482. Princeton University Press, Princeton, New Jersey.

Burnham, C.W., and Nekvasil, H. (1986) Equilibrium properties of granite pegmatite magmas. American Mineralogist, 71, 239–263.

Chernosky, J.V., Jr., Day, H.W., and Caruso, L.J. (1985) Equilibria in the system MgO-SiO_2-H_2O: Experimental determination of the stability of Mg-anthophyllite. American Mineralogist, 70, 223–236.

Circone, S., and Navrotsky, A. (1992) Substitution of $^{[6,4]}Al$ in phlogopite: High-temperature solution calorimetry, heat capacities, and thermodynamic properties of the phlogopite-eastonite join. American Mineralogist, 77, 1191–1205.

Clemens, J.D. (1990) The granulite-granite connexion. In D. Vielzeuf and P. Vidal, Eds., Granulites and crustal differentiation, p. 25–36. Kluwer Academic, Dordrecht, the Netherlands.

Clemens, J.D., and Vielzeuf, D. (1987) Constraints on melting and magma production in the crust. Earth and Planetary Science Letters, 86, 287–306.

Clemens, J.D., and Wall, V.J. (1981) Crystallization and origin of some peraluminous (S-type) granitic magmas. Canadian Mineralogist, 19, 111–131.

Clemens, J.D., Circone, S., Navrotsky, A., McMillan, P.F., Smith, B., and Wall, V.J. (1987) Phlogopite: New calorimetric data and the effect of stacking disorder on thermodynamic properties. Geochimica et Cosmochimica Acta, 51, 2569–2578.

Droop, G.T.R. (1994) Triple-chain pyriboles in Lewisian ultramafic rocks. Mineralogical Magazine, 58, 1–20.

Esperança, S., and Holloway, J.R. (1986) The origin of the high-K latites from Camp Creek, Arizona: Constraints from experiments with variable fO_2 and aH_2O. Contributions to Mineralogy and Petrology, 93, 504–512.

Forbes, W.C., and Fowler, M.F.J. (1974) Phase relations of titanphlogopite, $K_2Mg_4TiAl_2Si_6O_{20}(OH)_4$: A refractory phase in the upper mantle? Earth and Planetary Science Letters, 22, 92–97.

Fyfe, W.S. (1973) The granulite facies, partial melting and the Archean crust. Philosophical Transactions of the Royal Society of London, A273, 457–461.

Grant, J.A. (1986) Quartz-phlogopite-liquid equilibria and origins of charnockites. American Mineralogist, 71, 1071–1075.

Greenwood, H.J. (1963) The synthesis and stability field of anthophyllite, Journal of Petrology, 4, 317–351.

Hamilton, D.L., and Henderson, C.M.B. (1968) The preparation of silicate compositions by a gelling method. Mineralogical Magazine, 36, 832–838.

Helgeson, H.C., Delany, J.M., Nesbitt, H.W., and Bird, D.K. (1978) Summary and critique of the thermodynamic properties of rock-forming minerals. American Journal of Science, 278-A, 229.

Hoffer, E., and Grant, J.A. (1980) Experimental investigation of the formation of cordierite-orthopyroxene parageneses in pelitic rocks. Contributions to Mineralogy and Petrology, 73, 15–22.

Jakobsson, S., and Holloway, J.R. (1986) Crystal-liquid experiments in the presence of a C-O-H fluid buffered by graphite + iron + wustite: Experimental method and near-liquidus relations in basanite. Journal of Volcanology and Geothermal Research, 29, 265–291.

Johannes, W., and Holtz, F. (1990) Formation and composition of H_2O-undersaturated granitic melts. In J.R. Ashworth and M. Brown, Eds., High-temperature metamorphism and crustal anatexis, p. 87–104. Unwin Hyman, London.

Luth, W.C. (1967) Studies in the system $KAlSiO_4$-Mg_2SiO_4-SiO_2-H_2O: I. Inferred phase relations and petrologic application. Journal of Petrology, 8, 372–416.

Maaløe, S., and Wyllie, P.J. (1975) Water content of a granite magma deduced from the sequence of crystallization determined experimentally with water-undersaturated conditions. Contributions of Mineralogy and Petrology, 52, 175–191.

Montana, A., and Brearley, M. (1989) An appraisal of the stability of phlogopite in the crust and in the mantle. American Mineralogist, 74, 1–4.

Munoz, J.L., and Ludington, S.D. (1974) Fluorine-hydroxyl exchange in biotite. American Journal of Science, 274, 396–413.

Nekvasil, H., and Burnham, C.W. (1987) The calculated individual effects of pressure and water content on phase equilibria in the granite system. In B.O. Mysen, Ed., Magmatic processes: Physicochemical principles (Geochemical Society Special Publication 1), p. 433–445. Geochemical Society, University Park, Pennsylvania.

Nicholls, I.A. (1974) A direct fusion method of preparing rock glasses for energy-dispersive electron microprobe analysis. Chemical Geology, 14, 151–157.

O'Neill, H.S.C. (1987) Quartz-fayalite-iron and quartz-fayalite-magnetite equilibria and the free energy of formation of fayalite (Fe_2SiO_4) and magnetite (Fe_3O_4). American Mineralogist, 72, 67–75.

Ostapenko, G.T., Gorogotskaya, L.I., Timoshkova, L.P., and Yakovlev, B.G. (1987) Experimental study of the reaction biotite + 3 quartz = 3 orthopyroxene + potash feldspar + water. Geochemistry International, 24, 35–44.

Patera, E.S., and Holloway, J.R. (1982) Experimental determination of the spinel-garnet boundary in a Martian mantle composition. Journal of Geophysical Research, 87 (suppl.), A31–A36.

Patiño Douce, A.E. (1993) Titanium substitution in biotite: An empirical

model with applications to thermometry, O_2 and H_2O barometries, and consequences for biotite stability. Chemical Geology, 108, 133–162.

Peterson, J.W., and Newton, R.C. (1987) Reversed biotite + quartz melting reactions. EOS, 68, 451.

——— (1988) Experimental constraints on the vapor-absent melting of phlogopite + quartz. EOS, 69, 498.

——— (1989) Reversed experiments on biotite-quartz-feldspar melting in the system KMASH: Implications for crustal anatexis. Journal of Geology, 97, 465–485.

Peterson, J.W., Chacko, T., and Kuehner, S.M. (1991) The effects of fluorine on the vapor-absent melting of phlogopite + quartz: Implications for deep-crustal processes. American Mineralogist, 76, 470–476.

Piwinskii, A.J. (1968) Experimental studies of igneous rock series, central Sierra Nevada batholith, California. Journal of Geology, 76, 548–570.

——— (1973a) Experimental studies of igneous rock series, central Sierra Nevada batholith, California: Part II. Neues Jahrbuch für Mineralogie Monatshefte, 193–215.

——— (1973b) Experimental studies of granitoids from the central and southern Coast Ranges, California. Tschermaks Mineralogisch-Petrographische Mitteilungen, 20, 107–130.

Piwinskii, A.J., and Wyllie, P.J. (1968) Experimental studies of igneous rock series: A zoned pluton in the Wallowa batholith, Oregon. Journal of Geology, 76, 205–234.

Robert, J.L. (1976) Titanium solubility in synthetic phlogopite solid solutions. Chemical Geology, 17, 195–212.

Robie, R.A., and Hemingway, B.S. (1984) Heat capacities and entropies of phlogopite ($KMg_3[AlSi_3O_{10}](OH)_2$) and paragonite ($NaAl_2[AlSi_3O_{10}](OH)_2$) between 5 and 900 K and estimates of the enthalpies and Gibbs free energies of formation. American Mineralogist, 69, 858–868.

Thompson, A.B. (1990) Heat, fluids and melting in the granulite facies. In D. Vielzeuf and P. Vidal, Eds., Granulites and crustal differentiation, p. 37–58. Kluwer Academic, Dordrecht, the Netherlands.

Tronnes, R.G., Edgar, A.D., and Arima, M. (1985) A high pressure–high temperature study of TiO_2 solubility in Mg-rich phlogopites: Implication to phlogopite chemistry. Geochimica et Cosmochimica Acta, 49, 2323–2329.

Vielzeuf, D., and Clemens, J.D. (1992) The fluid-absent melting of phlogopite + quartz: Experiments and models. American Mineralogist, 77, 1206–1222.

Vielzeuf, D., and Montel, J.-M. (1994) Partial melting of metagreywackes: 1. Fluid-absent experiments and phase relationships. Contributions to Mineralogy and Petrology, 117, 375–393.

Vielzeuf D., Clemens, J.D. and Pin, C. (1990) Granites, granulites and crustal differentiation. In D. Vielzeuf and P. Vidal, Eds., Granulites and crustal differentiation, p. 59–86. Kluwer Academic, Dordrecht, the Netherlands.

White, A.J.R., and Chappell, B.W. (1977) Ultrametamorphism and granitoid genesis. Tectonophysics, 43, 7–22.

Wones, D.R., and Dodge, F.C.W. (1977) The stability of phlogopite in the presence of quartz and diopside. In D.G. Fraser, Ed., Thermodynamics in geology, p. 229–247. Reidel, Dordrecht, the Netherlands.

Wood, B.J. (1976) The reaction phlogopite + quartz = enstatite + sanidine + H_2O. Progress in Experimental Petrology, 6, 17–19.

Wright, T.L. (1968) X-ray and optical study of alkali feldspar: II. An X-ray method for determining the composition and structural state from measurement of 2θ values for three reflections. American Mineralogist, 53, 88–104.

Manuscript received December 8, 1994
Manuscript accepted May 15, 1995